Supplement of Weather Clim. Dynam., 7, 979–1007, 2026
https://doi.org/10.5194/wcd-7-979-2026-supplement

Supplement of

Global monsoon in ICON: the scale-dependent response of Northern Hemisphere monsoons

Praveen K. Pothapakula et al.

Correspondence to: Praveen K. Pothapakula (praveen.pothapakula@env.ethz.ch)

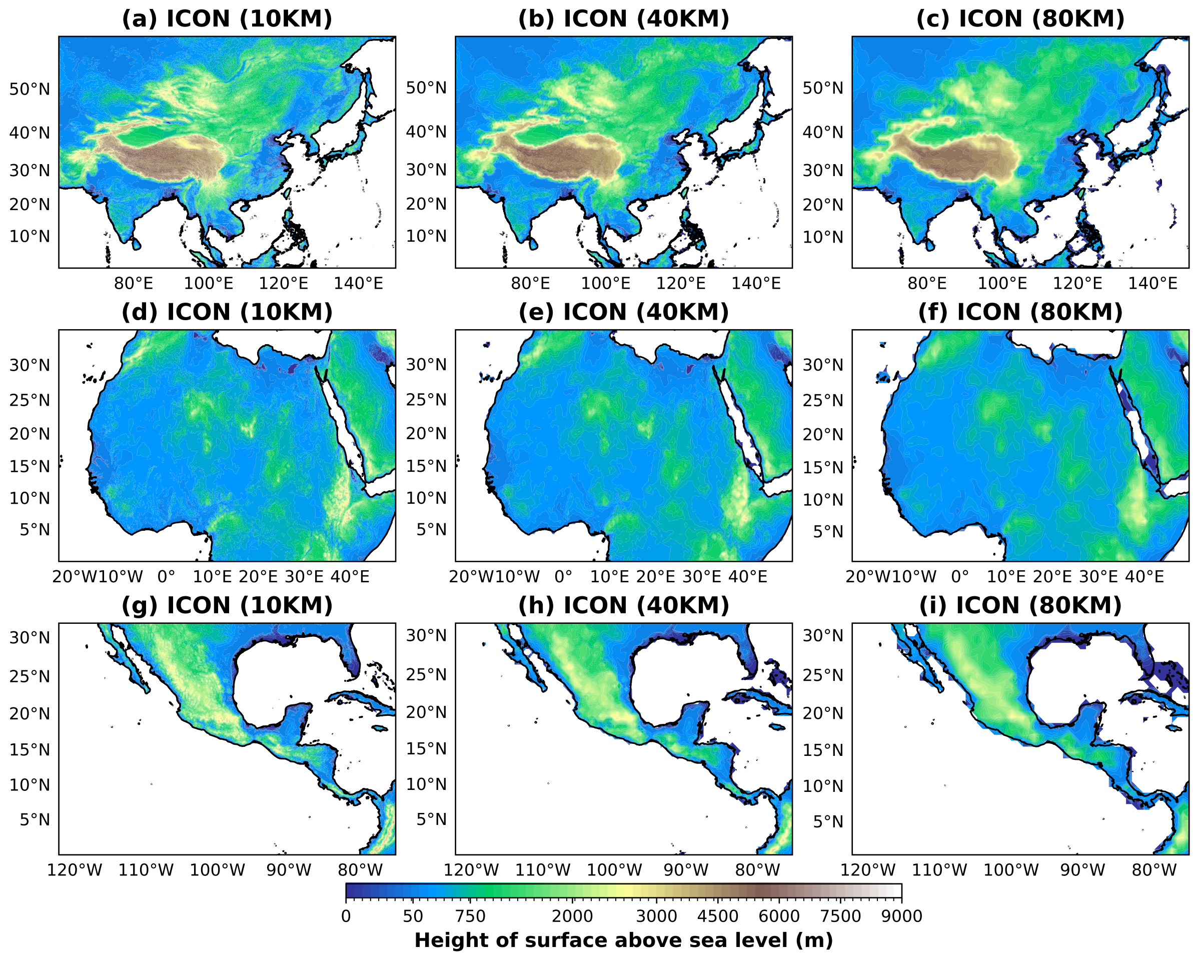

Figure S1: Topography of Northern Hemisphere monsoon domains in various ICON simulations at 10 km, 40 km, and 80 km grid spacings.(a-c) SAsiaM domain (d-f) WAfriM domain and (g-h) NAmerM domain

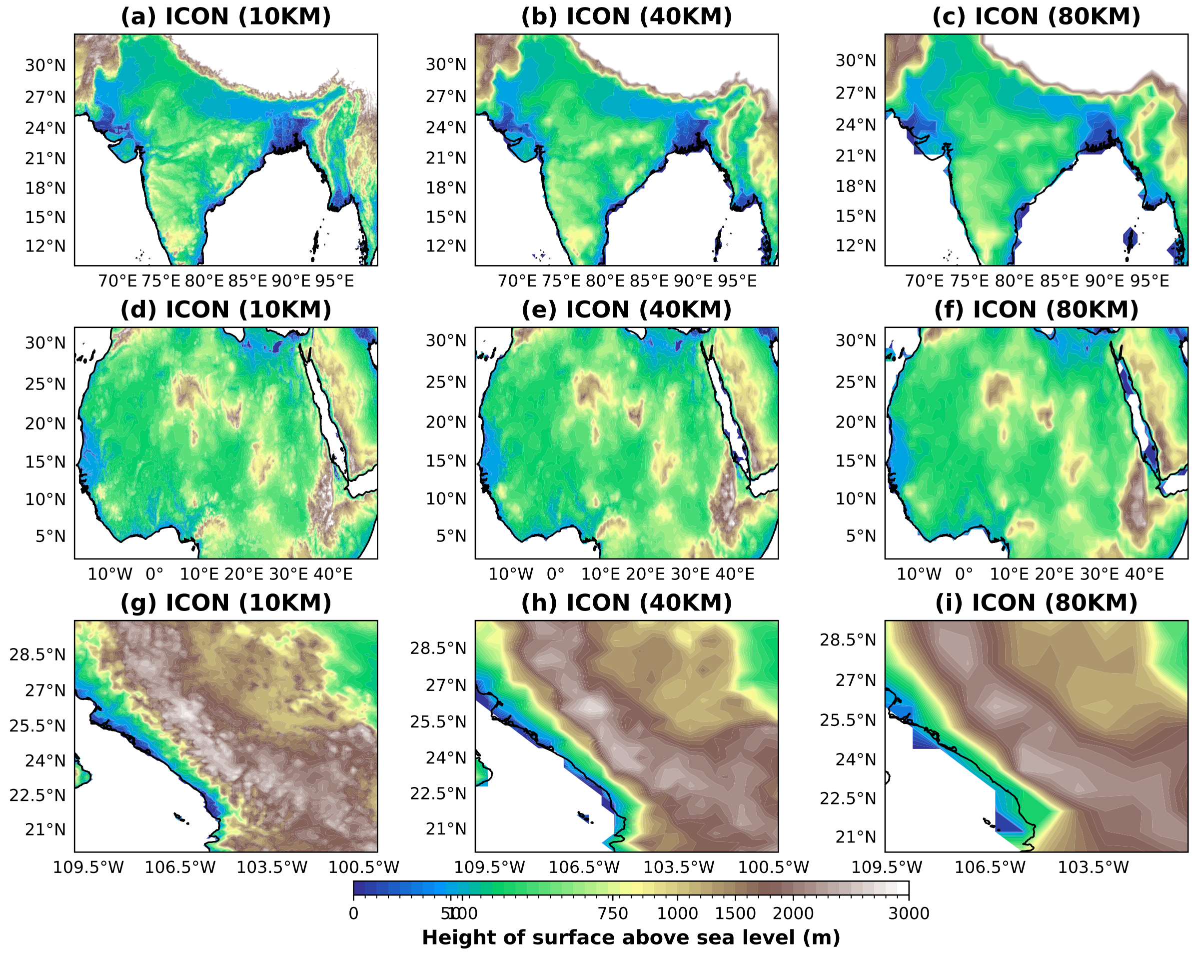

Figure S2: Topography zoomed over Northern Hemisphere monsoon domains in various ICON simulations at 10 km, 40 km, and 80 km grid spacings.(a-c) SAsiaM domain (d-f) WAfriM domain and (g-h) NAmerM domain. The figure illustrates that fine grid spacing better resolves the complex features in these domains compared to its coarser counter part.

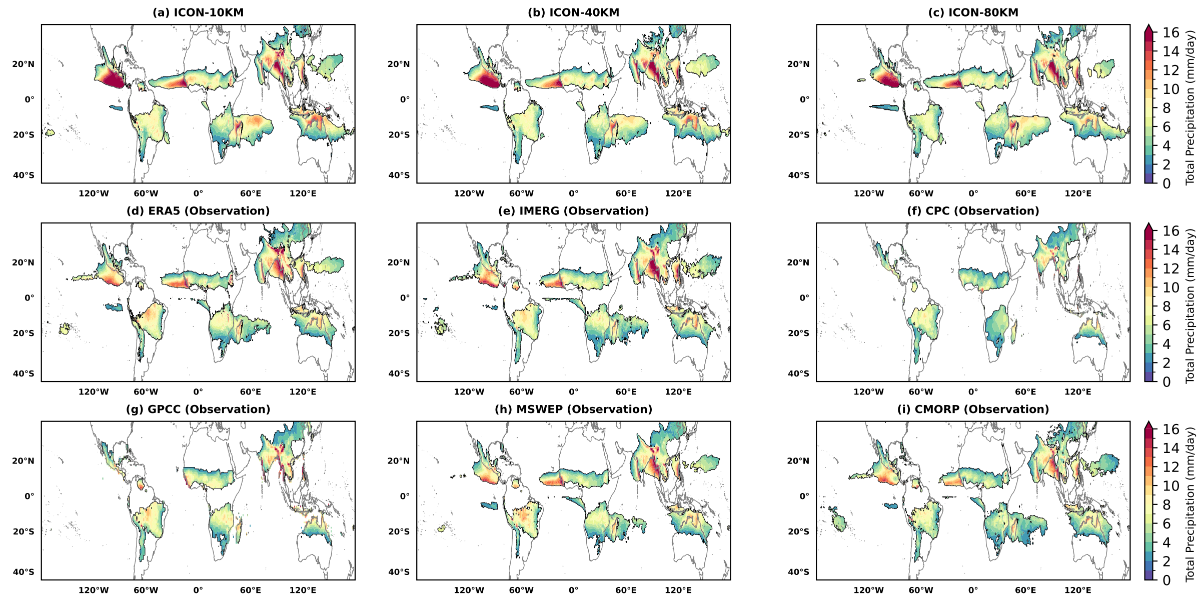

Figure S3: Global monsoon domains (contours), defined by regions where local summer minus winter precipitation $> 2\,\mathrm{mm/day}$ and local summer precipitation $\geq 55\,\%$ of annual total precipitation. The shaded regions show the annual range (summer minus winter) in (a-c) ICON simulations at 10 km, 40 km, and 80 km resolution, and six observational datasets (d-e) for a period of 10 years (2007-2016).

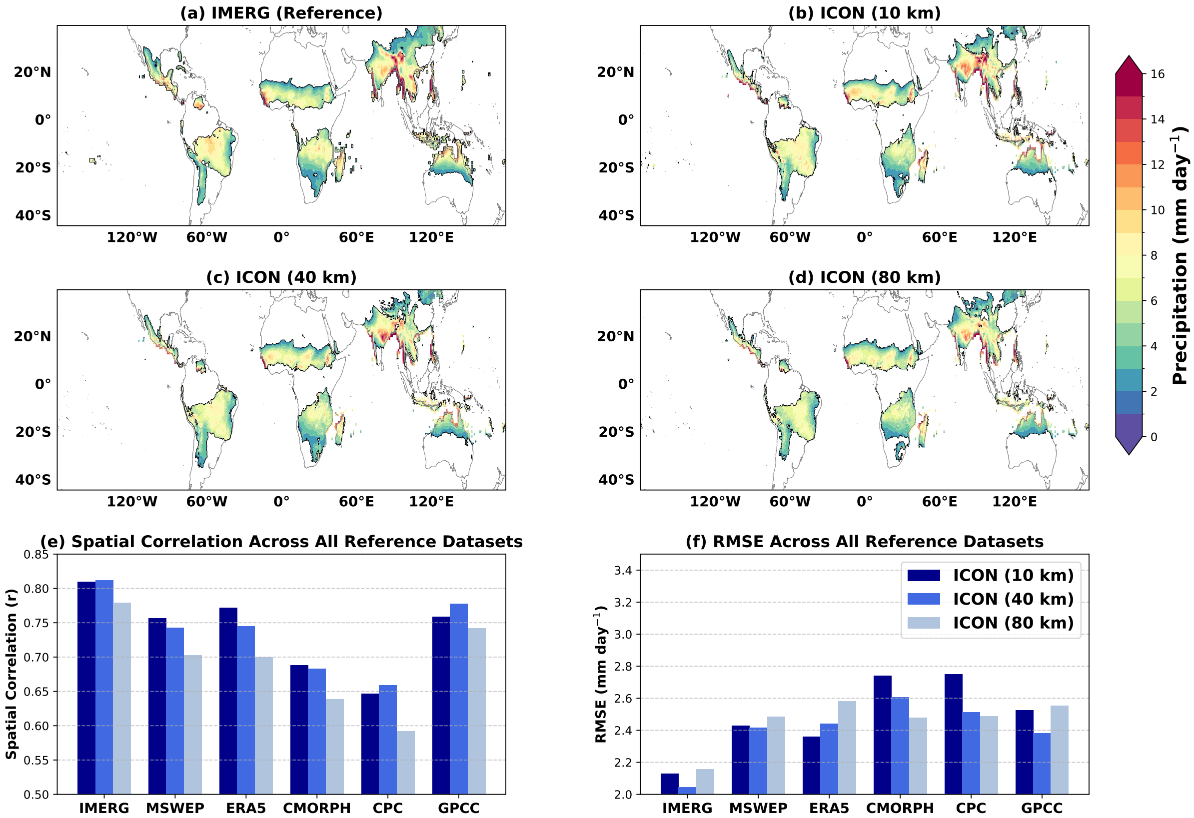

Figure S4: Global monsoon domains over the land regions (contours), defined by regions where local summer minus winter precipitation difference > 2 mm/day and summer precipitation contribution ≥ 55 % of annual total. The shaded regions show the annual range of precipitation (local summer minus winter) in (a) IMERG observations and (b-d) ICON simulations at 10 km, 40 km, and 80 km grid spacing. (e) Spatial correlation and (f) RMSE of the monsoon precipitation annual range for ICON simulations against six observational datasets (2007-2016). The spatial correlation and RMSE values are statistically significant ($p < 0.05$) with students t-test. All the datasets are plotted and analyzed at a common grid, with grid spacing of 30 km.

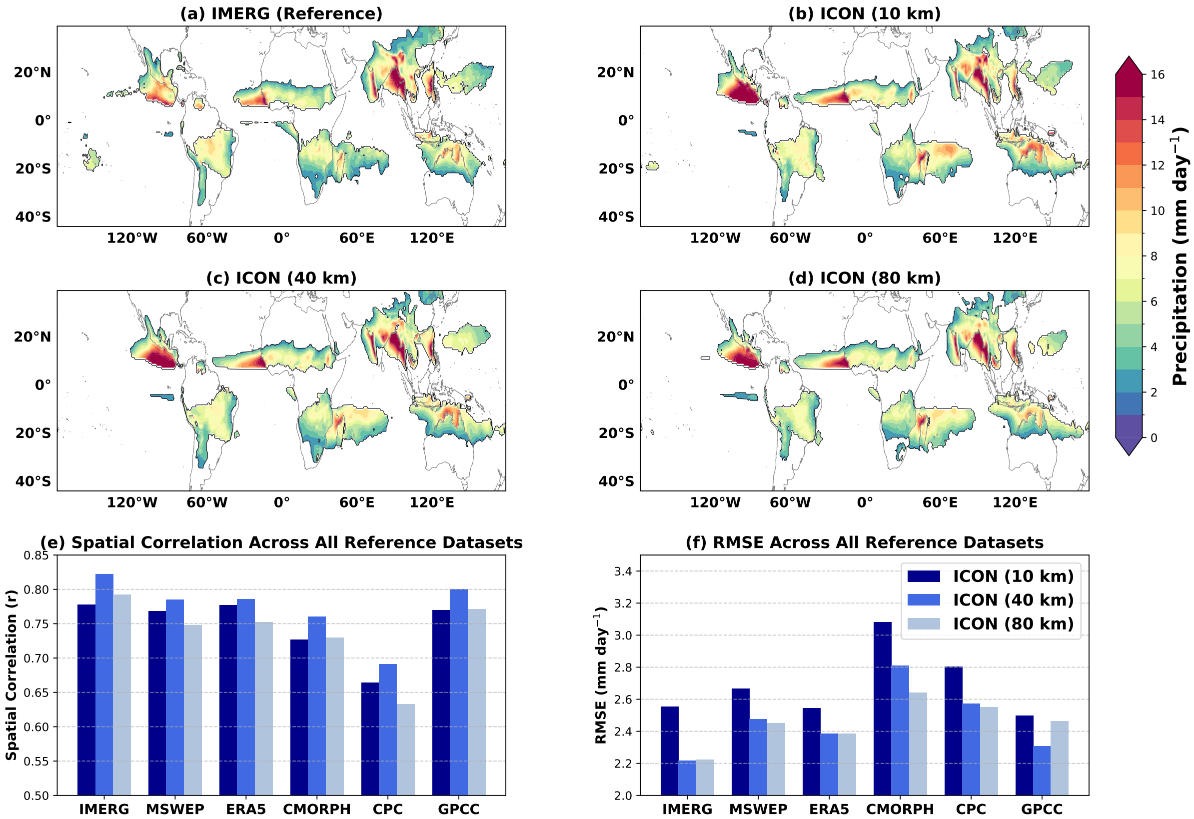

Figure S5: Global monsoon domains (contours), defined by regions where local summer minus winter precipitation difference > 2 mm/day and summer precipitation contribution $\geq 55\,\%$ of annual total. The shaded regions show the annual range of precipitation (local summer minus winter) in (a) IMERG observations and (b-d) ICON simulations at 10 km, 40 km, and 80 km grid spacing. (e) Spatial correlation and (f) RMSE of the monsoon precipitation annual range for ICON simulations against six observational datasets (2007-2016). The spatial correlation and RMSE values are statistically significant ($p < 0.05$) with students t-test. All the datasets are plotted and analyzed at a common grid, with grid spacing of 80 km.

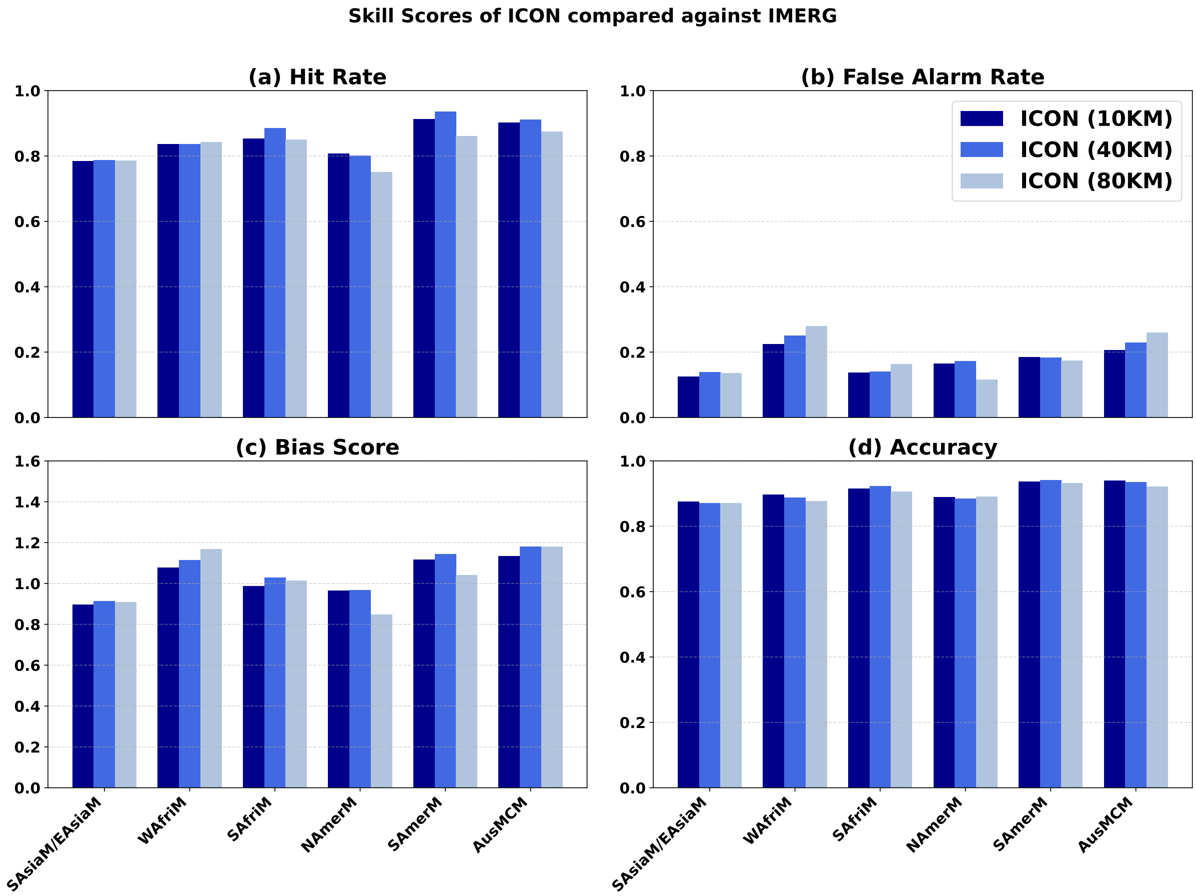

Figure S6: Performance assessment of ICON simulations in reproducing the monsoon domain boundaries shown in Fig. 2 against the IMERG reference. The panel (a) displays the Hit Rate (probability of detection) (b) False Alarm Rate (probability of false detection) (c) displays the Bias (frequency ratio), indicating the simulation's tendency to over or under-predict the domain, and (d) the Accuracy (fraction correct), representing the overall proportion of correct detections.

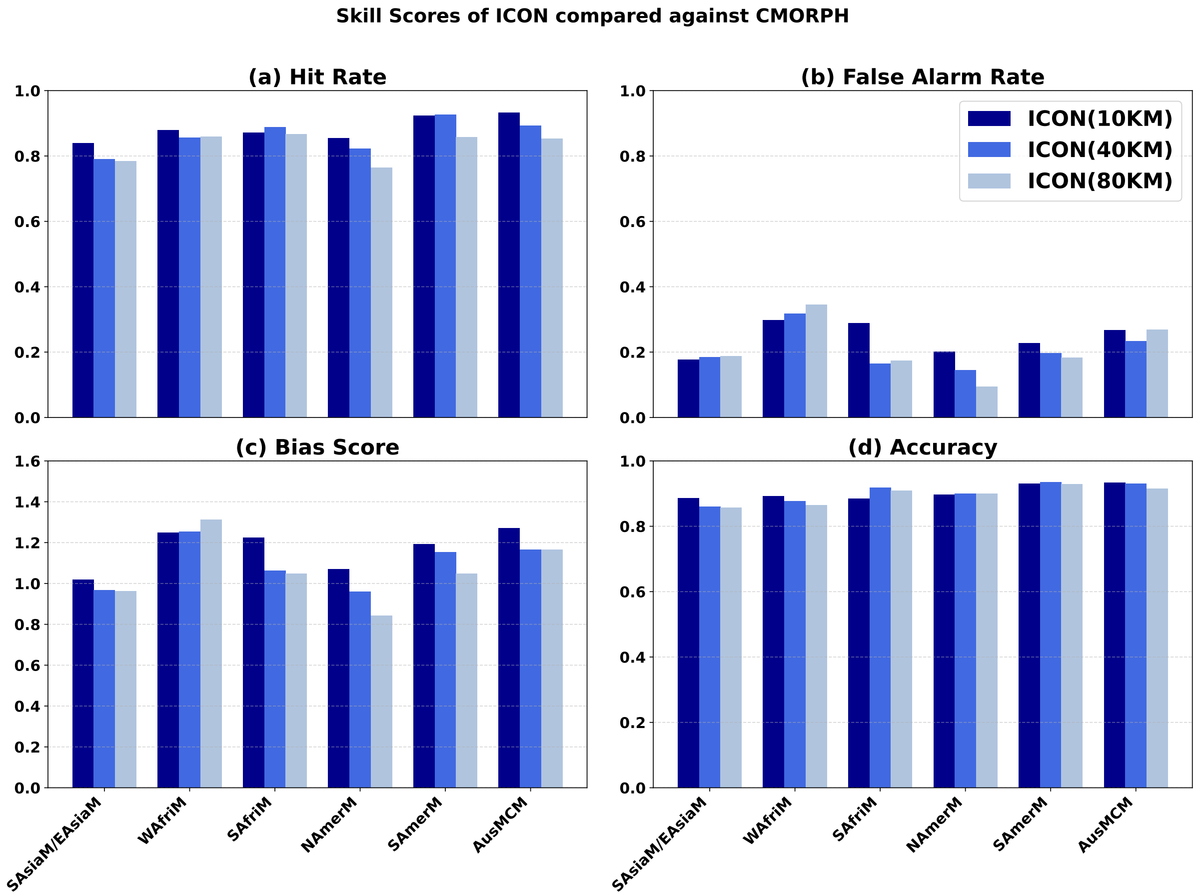

Figure S7: Performance assessment of ICON simulations in reproducing the monsoon domain boundaries shown in Fig. 2 against the CMOPRH reference. The panel (a) displays the Hit Rate (probability of detection) (b) False Alarm Rate (probability of false detection) (c) displays the Bias (frequency ratio), indicating the simulation's tendency to over or under-predict the domain, and (d) the Accuracy (fraction correct), representing the overall proportion of correct detections.

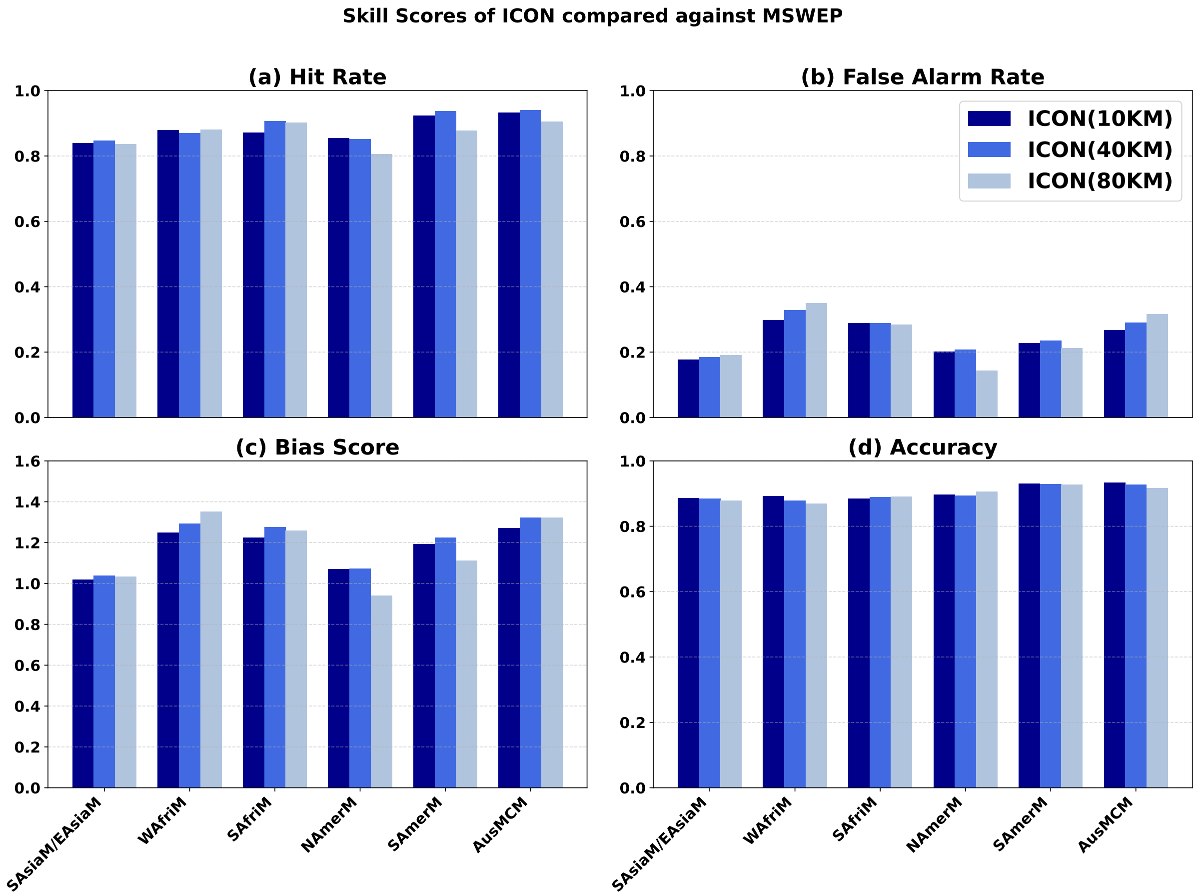

Figure S8: Performance assessment of ICON simulations in reproducing the monsoon domain boundaries shown in Fig. 2 against the MSWEP reference. The panel (a) displays the Hit Rate (probability of detection) (b) False Alarm Rate (probability of false detection) (c) displays the Bias (frequency ratio), indicating the simulation's tendency to over or under-predict the domain, and (d) the Accuracy (fraction correct), representing the overall proportion of correct detections.

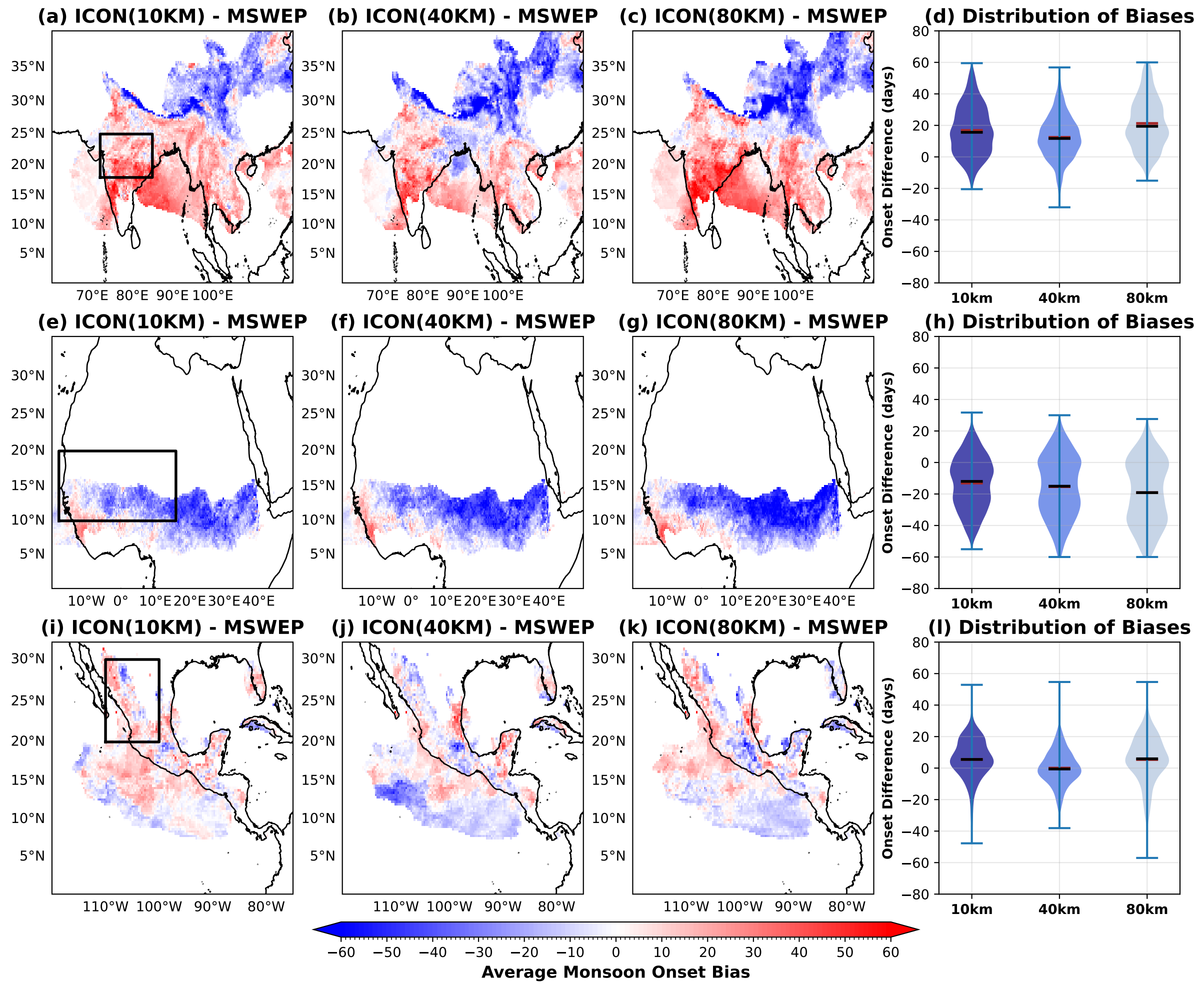

Figure S9: Spatial patterns of mean bias in the monsoon onset during the summer monsoon season (JJAS) in various ICON model simulations with reference to MSWEP dataset for (a-d) the SAsiaM domain, (e-h) WAfriM, and (i-l) NAmerM. The black boxes in the SAsiaM (a), WAfriM (e) and NAmerM (i) domains indicate the respective core monsoon regions, and the violin plots show the bias distribution of the monsoon onset day over the highlighted box regions. The black bar in the violin plots indicate the median, while the brown bar indicates the mean bias in monsoon onset over the monsoon core regions.

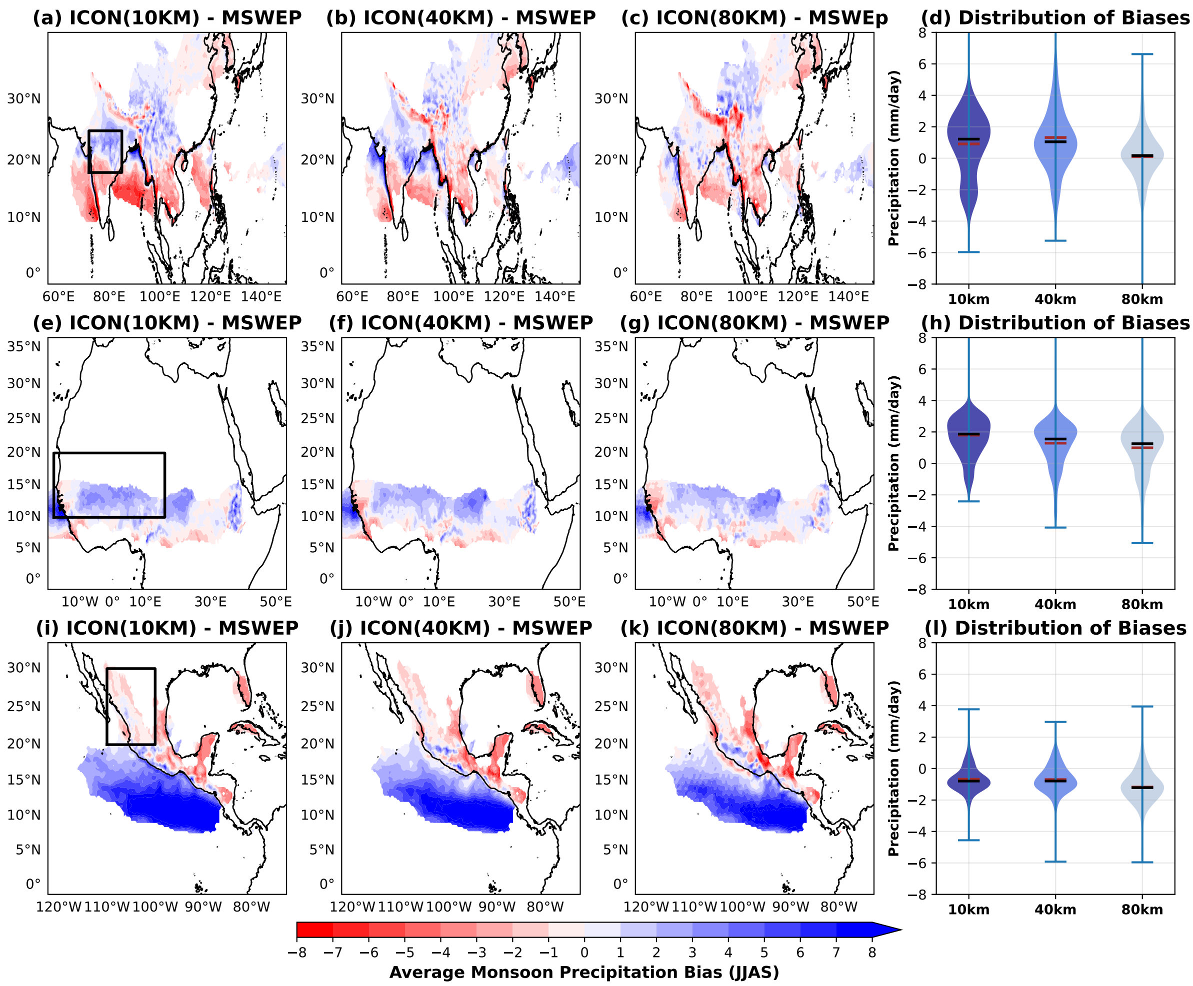

Figure S10: Spatial patterns of the mean bias in the total precipitation occurring during the summer monsoon season (JJAS) in various ICON simulations with reference MSWEP dataset over the SAsiaM (a-d), the WAfriM (e-h), and the NAmerM (i-l) domains respectively. The black boxes in the SAsiaM (a), WAfriM (e) and NAmerM (i) domains indicate the respective core monsoon regions, and the violin plots show the bias distribution of total precipitation over the highlighted box regions. The black bar in the violin plots indicate the median, while the brown bar indicates the mean of the total precipitation bias.

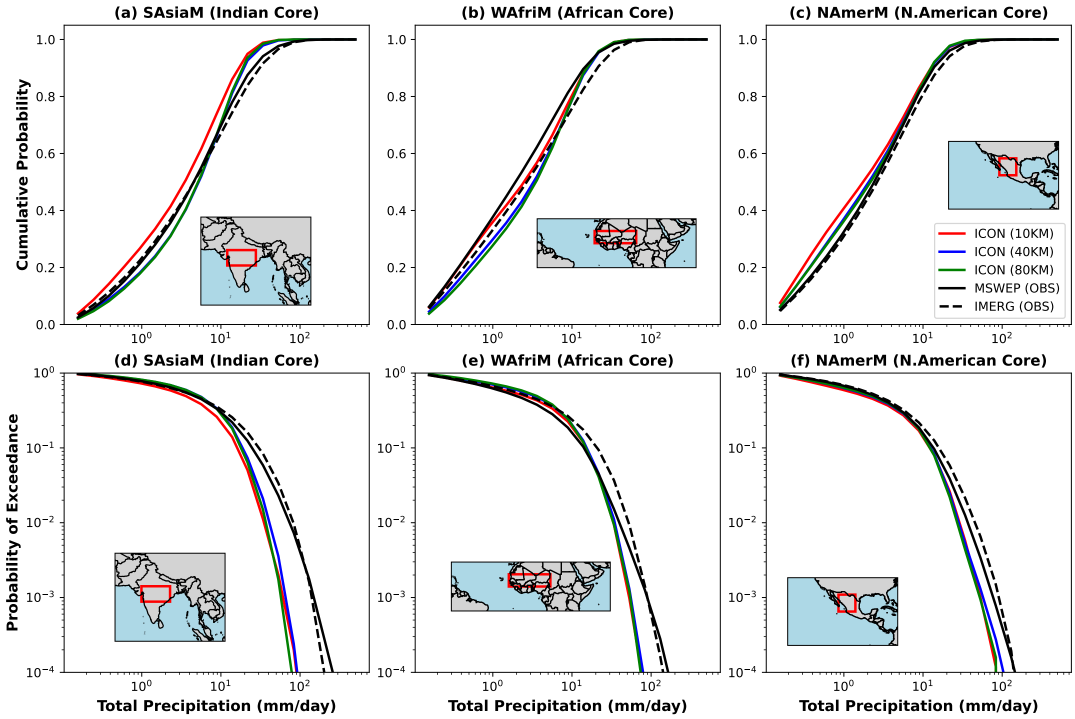

Figure S11: Cumulative probability distribution of daily convective precipitation over the SAsiaM, WAfriM, and NAmerM core regions (red boxes) during local summer monsoon season (JJAS). The top row (a-c) shows the cumulative probability distribution function on a linear probability scale, highlighting biases in light to moderate convective rainfall frequency. The bottom panel (d-f) shows the complementary cumulative distribution function, or probability of exceedance on a logarithmic probability scale to emphasize on the extreme precipitation. The IMERG and MSWEP total precipitation observational datasets (in solid and dotted black lines respectively) are used to qualitatively compare against ICON model convective precipitation contributions.

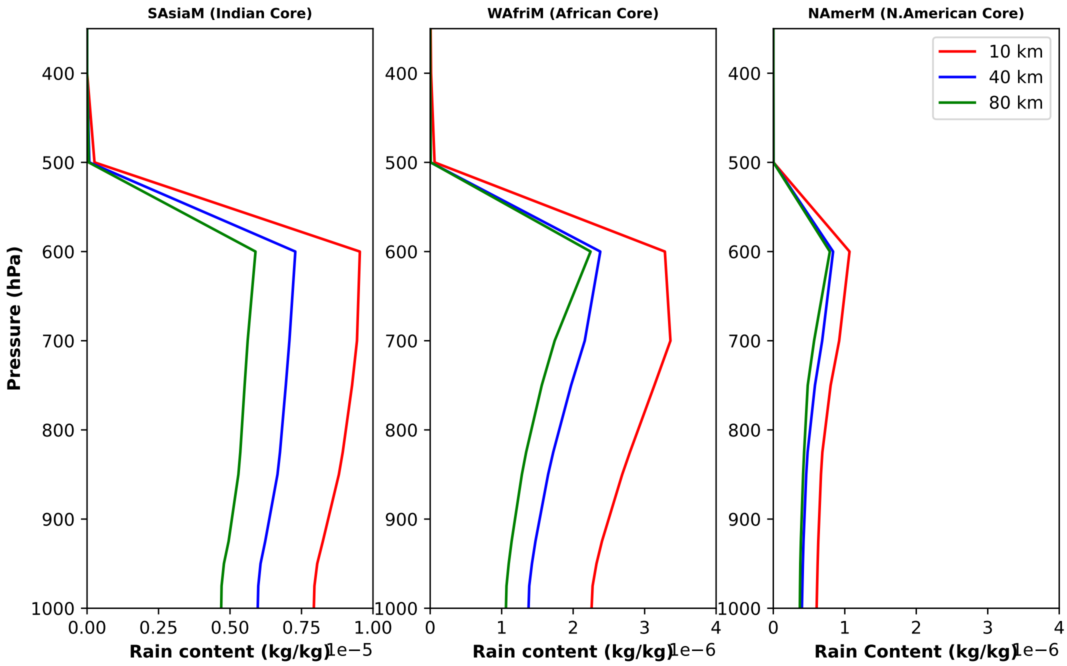

Figure S12: Sensitivity of rain content (kg/kg) to grid spacing in ICON 10 km, 40 km, and 80 km simulations for the SAsiaM, WAfriM, and NAmerM core domains. The cloud water is averaged over the respective monsoon core regions and is plotted against pressure levels level. All the simulations are brought to a common 30 km grid for analysis. The rain content increases with fine grid spacing, while the cloud water (kg/kg) decreases in the lower troposphere, enhancing the cloud microphysical efficiency.

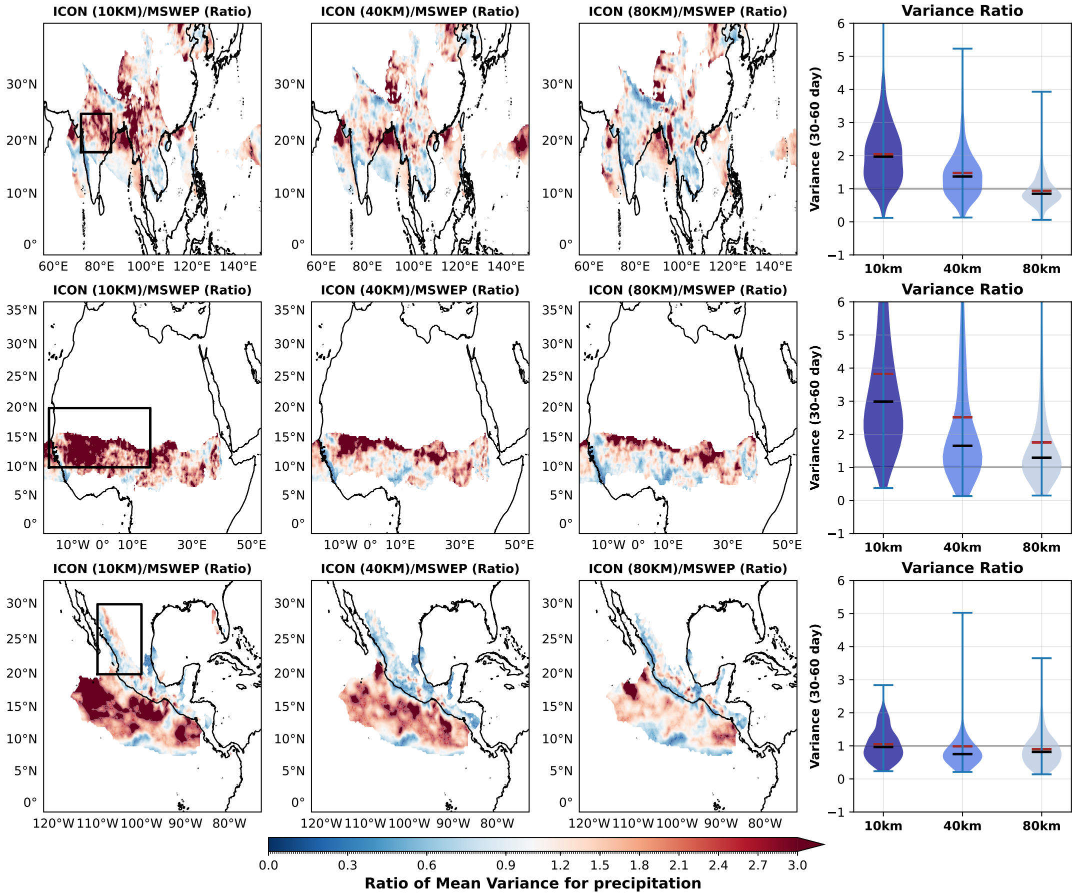

Figure S13: The Spatial patterns of 30–90 day filtered precipitation variance of ICON divided by the variance of MSWEP during summer monsoon season (JJAS) representing intraseasonal variability. The top panel shows the ratio of variance for SAsiaM domain, while the region highlighted in the black box represents core monsoon region. Similarly the middle and the bottom panel show WAfriM and NAmerM domains respectively with black box indicating the core monsoon regions. The violin plot on the right most panels show distribution of the variance ratio's in the core monsoon domains, with black bar indicating the median, while the brown bar indicates the mean of the distribution.

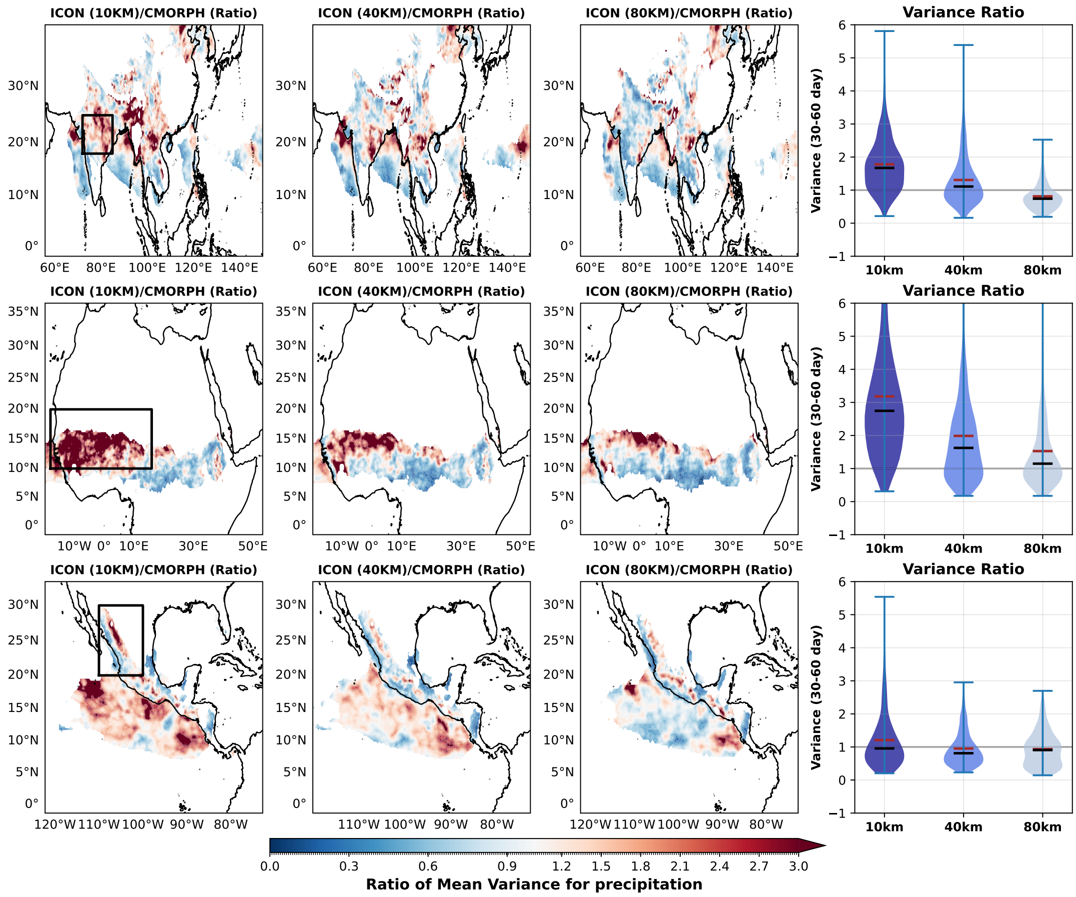

Figure S14: The Spatial patterns of 30–90 day filtered precipitation variance of ICON divided by the variance of CMORPH during summer monsoon season (JJAS) representing intraseasonal variability. The top panel shows the ratio of variance for SAsiaM domain, while the region highlighted in the black box represents core monsoon region. Similarly the middle and the bottom panel show WAfriM and NAmerM domains respectively with black box indicating the core monsoon regions. The violin plot on the right most panels show distribution of the variance ratio's in the core monsoon domains, with black bar indicating the median, while the brown bar indicates the mean of the distribution.

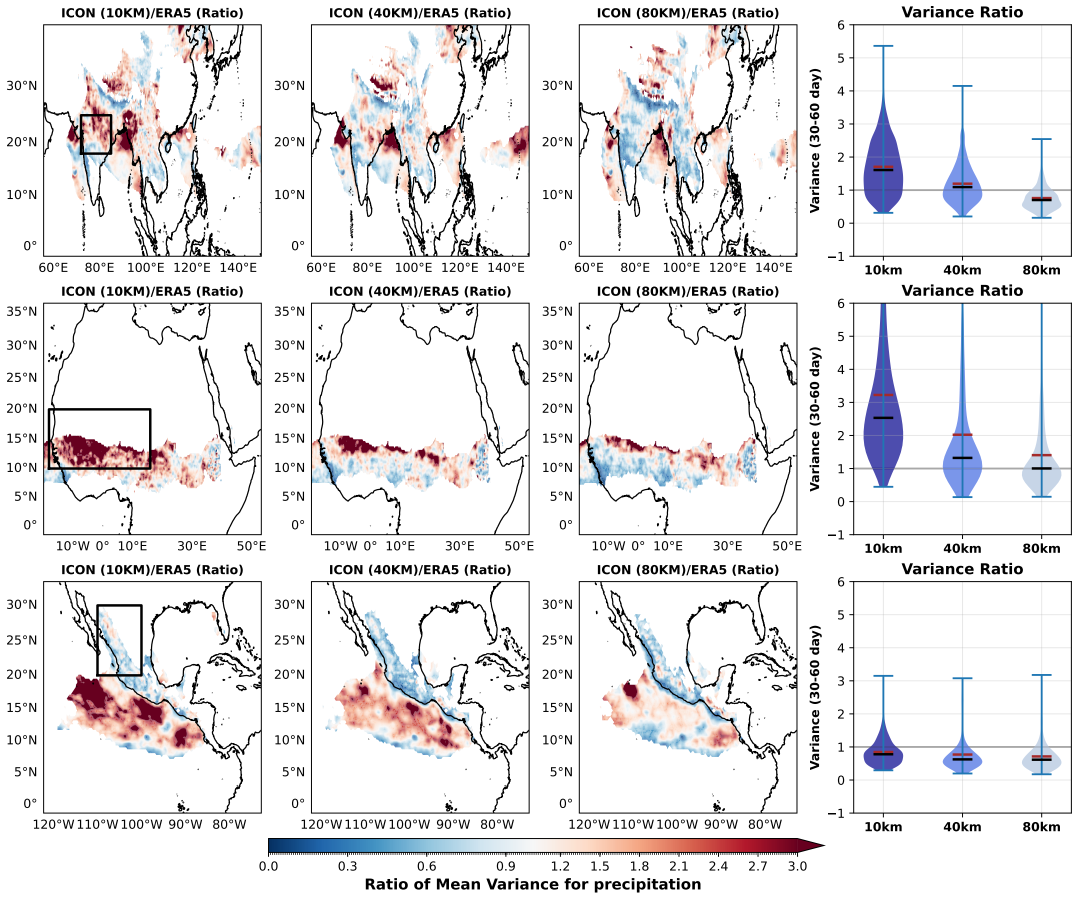

Figure S15: The Spatial patterns of 30–90 day filtered precipitation variance of ICON divided by the variance of ERA5 during summer monsoon season (JJAS) representing intraseasonal variability. The top panel shows the ratio of variance for SAsiaM domain, while the region highlighted in the black box represents core monsoon region. Similarly the middle and the bottom panel show WAfriM and NAmerM domains respectively with black box indicating the core monsoon regions. The violin plot on the right most panels show distribution of the variance ratio's in the core monsoon domains, with black bar indicating the median, while the brown bar indicates the mean of the distribution.

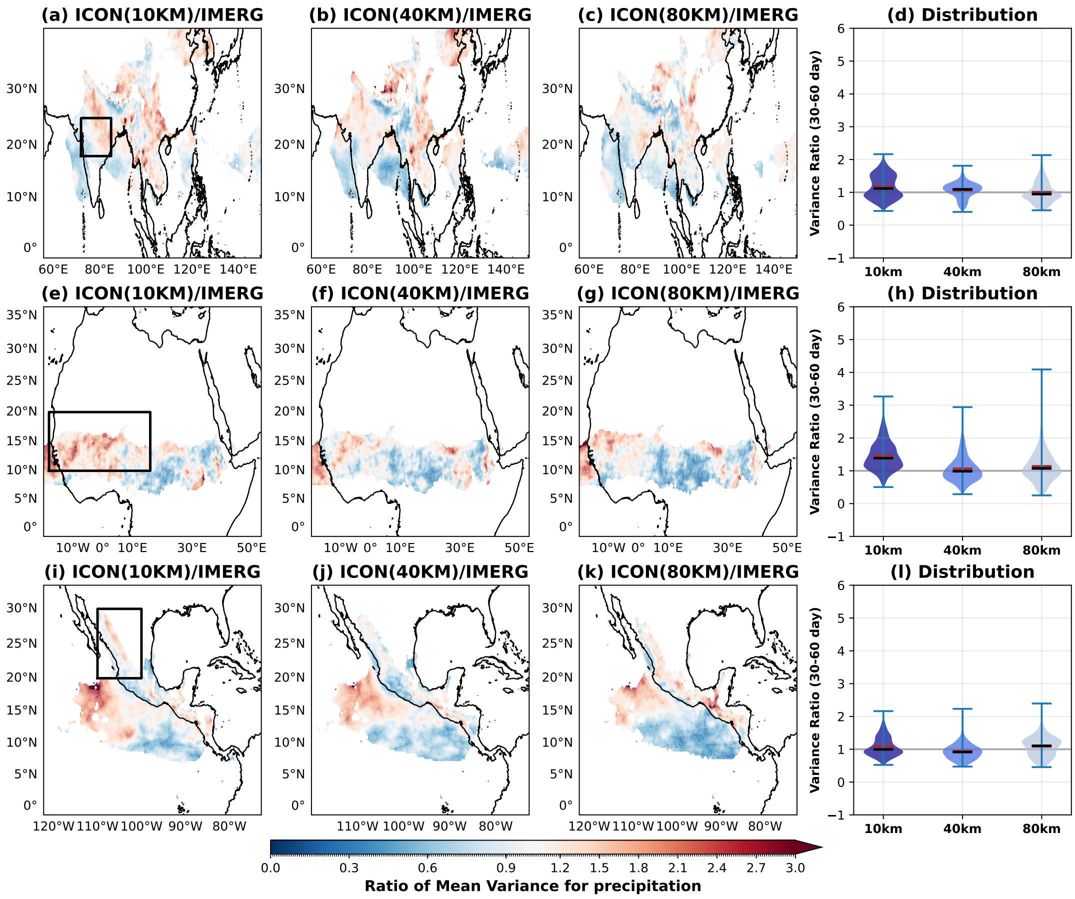

Figure S16: The Spatial patterns of 30–90 day filtered precipitation (transformed with log(1+P)) variance of ICON divided by the variance of IMERG during summer monsoon season (JJAS) representing intraseasonal variability. The top panel shows the ratio of variance for SAsiaM domain, while the region highlighted in the black box represents core monsoon region. Similarly the middle and the bottom panel show WAfriM and NAmerM domains respectively with black box indicating the core monsoon regions. The violin plot on the right most panels show distribution of the variance ratio's in the core monsoon domains, with black bar indicating the median, while the brown bar indicates the mean of the distribution.

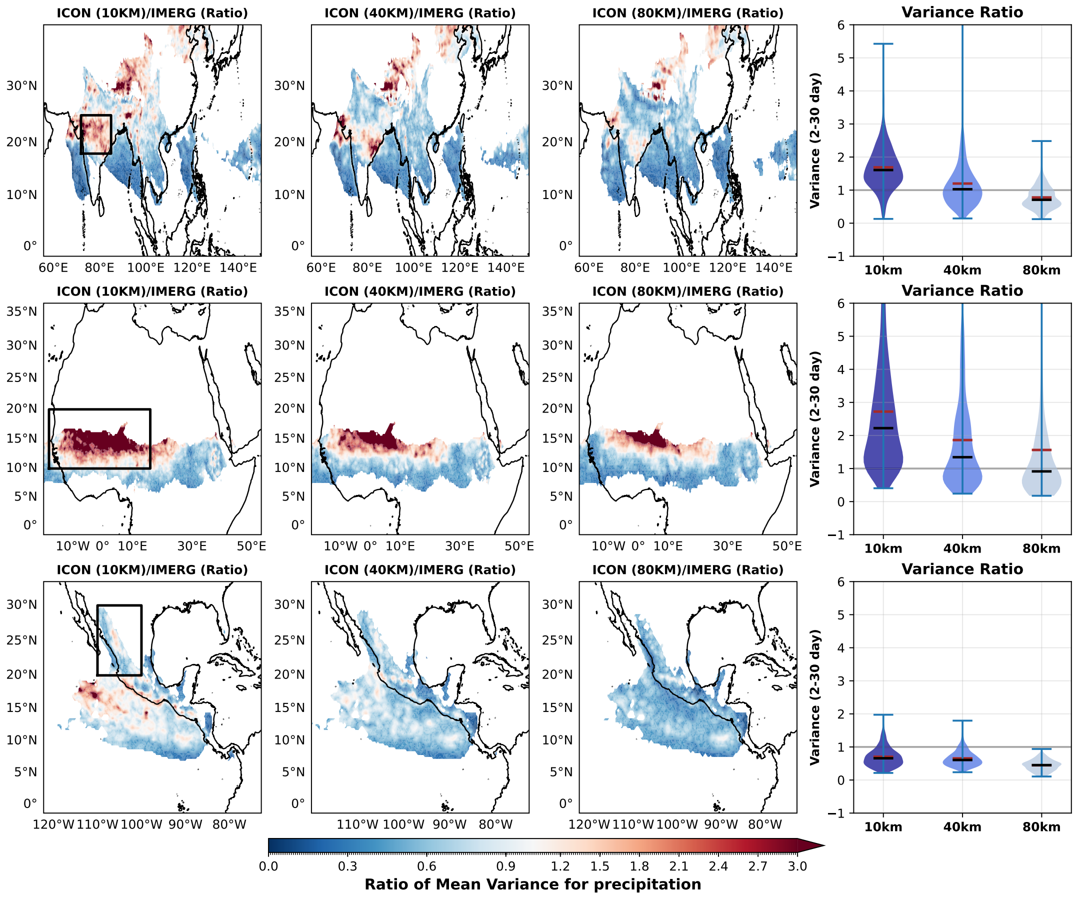

Figure S17: The Spatial patterns of 2–30 day filtered precipitation variance of ICON divided by the variance of IMERG during summer monsoon season (JJAS) representing intraseasonal variability. The top panel shows the ratio of variance for SAsiaM domain, while the region highlighted in the black box represents core monsoon region. Similarly the middle and the bottom panel show WAfriM and NAmerM domains respectively with black box indicating the core monsoon regions. The violin plot on the right most panels show distribution of the variance ratio's in the core monsoon domains, with black bar indicating the median, while the brown bar indicates the mean of the distribution.

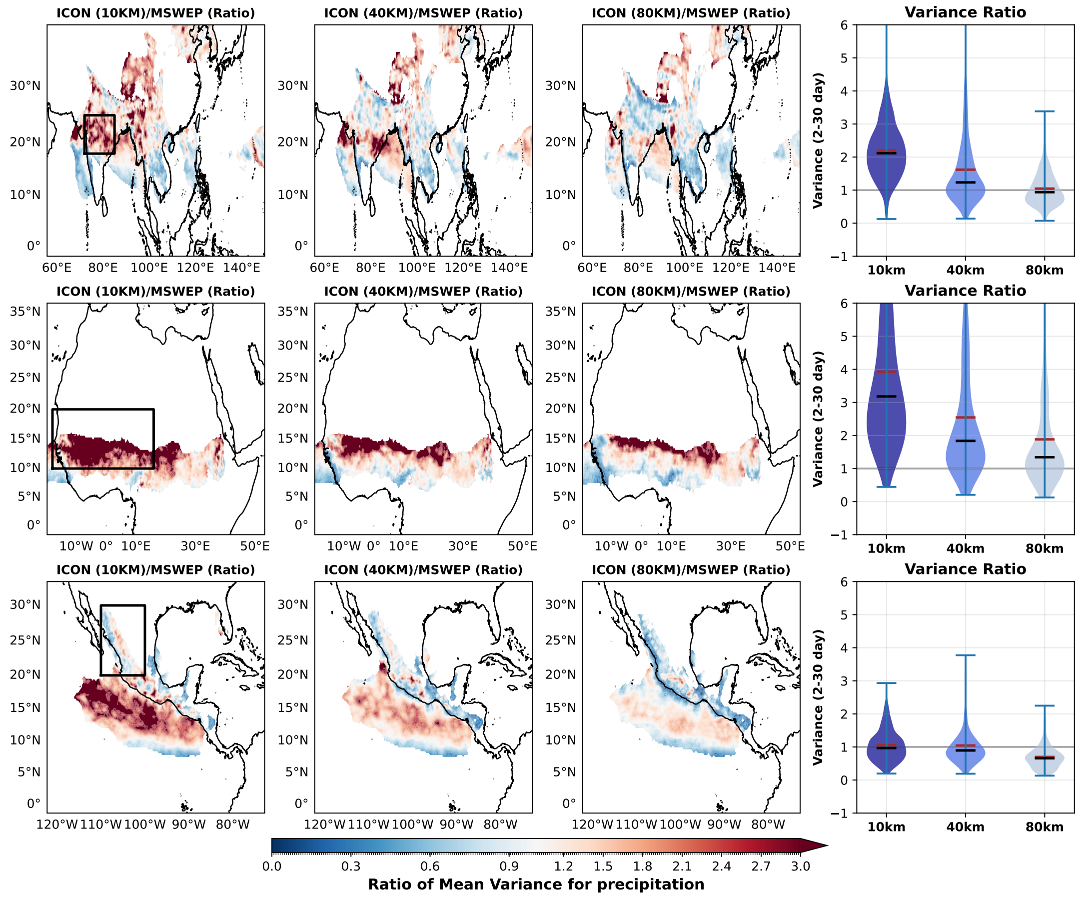

Figure S18: The Spatial patterns of 2–30 day filtered precipitation variance of ICON divided by the variance of MSWEP during summer monsoon season (JJAS) representing intraseasonal variability. The top panel shows the ratio of variance for SAsiaM domain, while the region highlighted in the black box represents core monsoon region. Similarly the middle and the bottom panel show WAfriM and NAmerM domains respectively with black box indicating the core monsoon regions. The violin plot on the right most panels show distribution of the variance ratio's in the core monsoon domains, with black bar indicating the median, while the brown bar indicates the mean of the distribution.

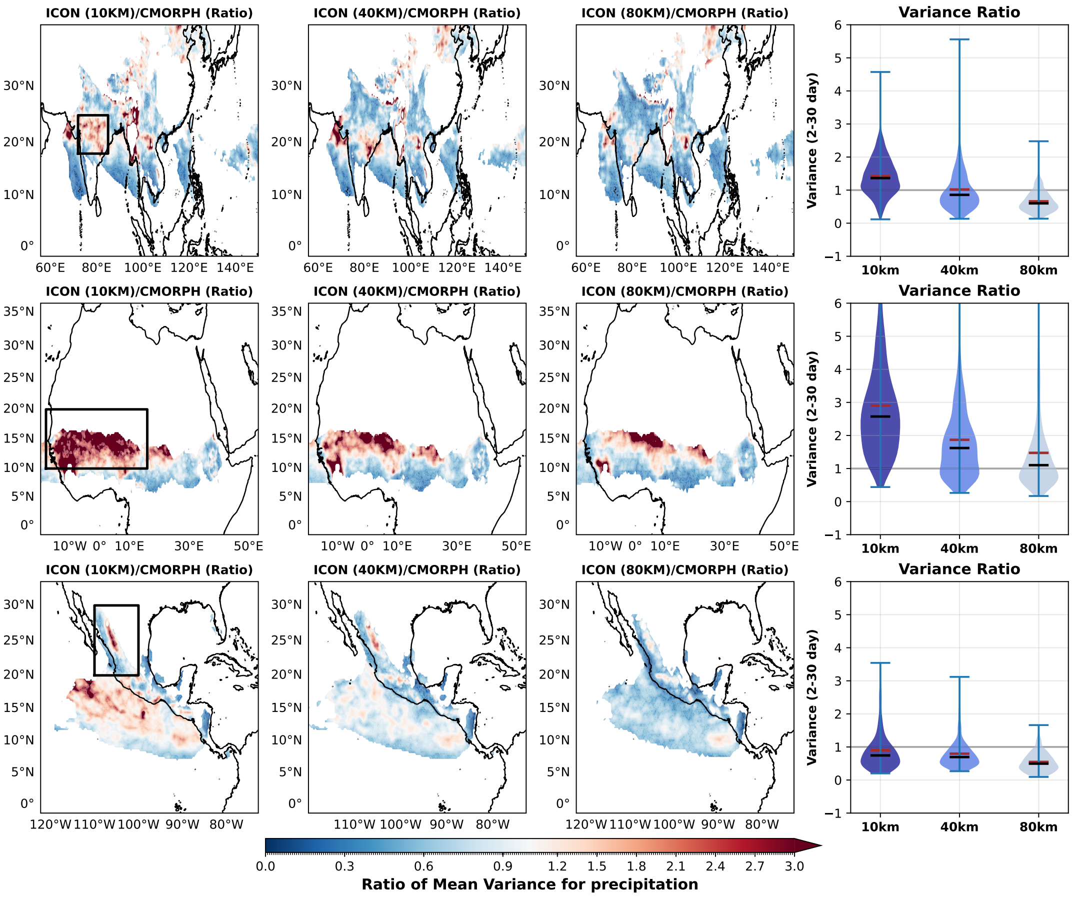

Figure S19: The Spatial patterns of 2–30 day filtered precipitation variance of ICON divided by the variance of CMORPH during summer monsoon season (JJAS) representing intraseasonal variability. The top panel shows the ratio of variance for SAsiaM domain, while the region highlighted in the black box represents core monsoon region. Similarly the middle and the bottom panel show WAfriM and NAmerM domains respectively with black box indicating the core monsoon regions. The violin plot on the right most panels show distribution of the variance ratio's in the core monsoon domains, with black bar indicating the median, while the brown bar indicates the mean of the distribution.

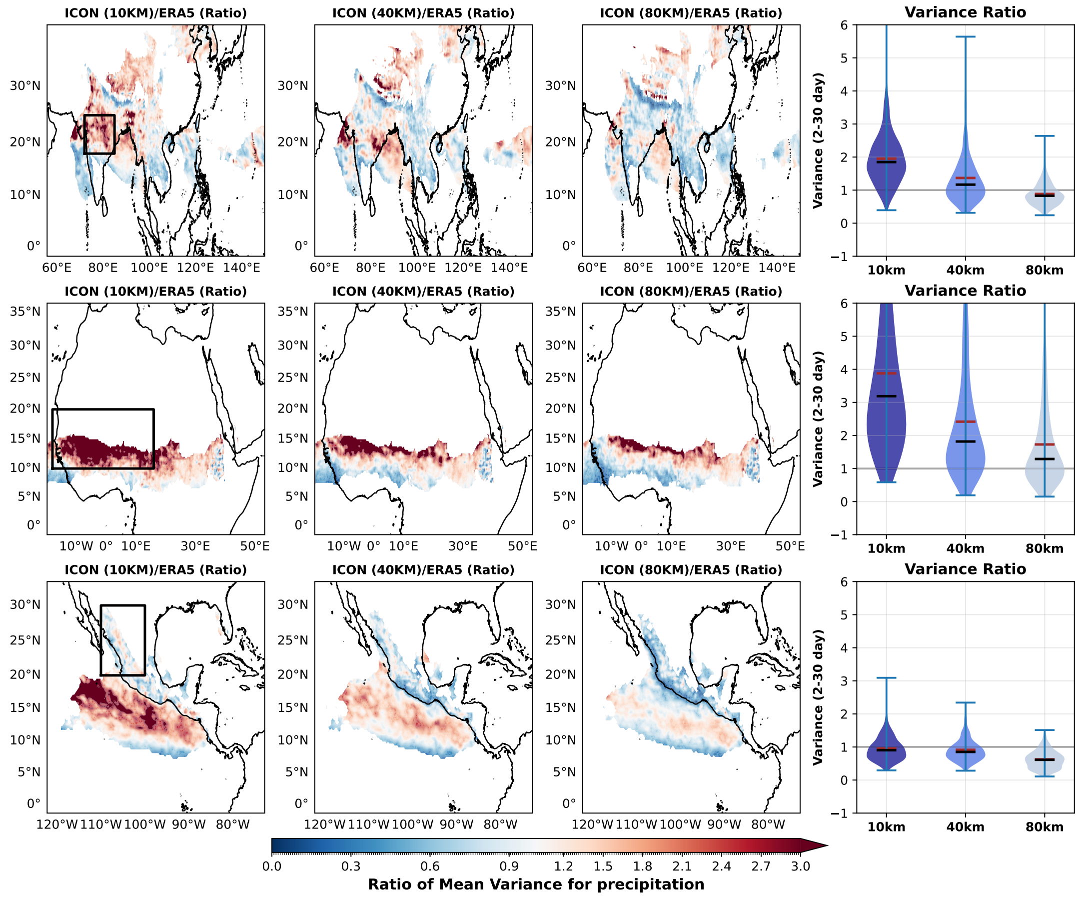

Figure S20: The Spatial patterns of 2–30 day filtered precipitation variance of ICON divided by the variance of ERA5 during summer monsoon season (JJAS) representing intraseasonal variability. The top panel shows the ratio of variance for SAsiaM domain, while the region highlighted in the black box represents core monsoon region. Similarly the middle and the bottom panel show WAfriM and NAmerM domains respectively with black box indicating the core monsoon regions. The violin plot on the right most panels show distribution of the variance ratio's in the core monsoon domains, with black bar indicating the median, while the brown bar indicates the mean of the distribution.

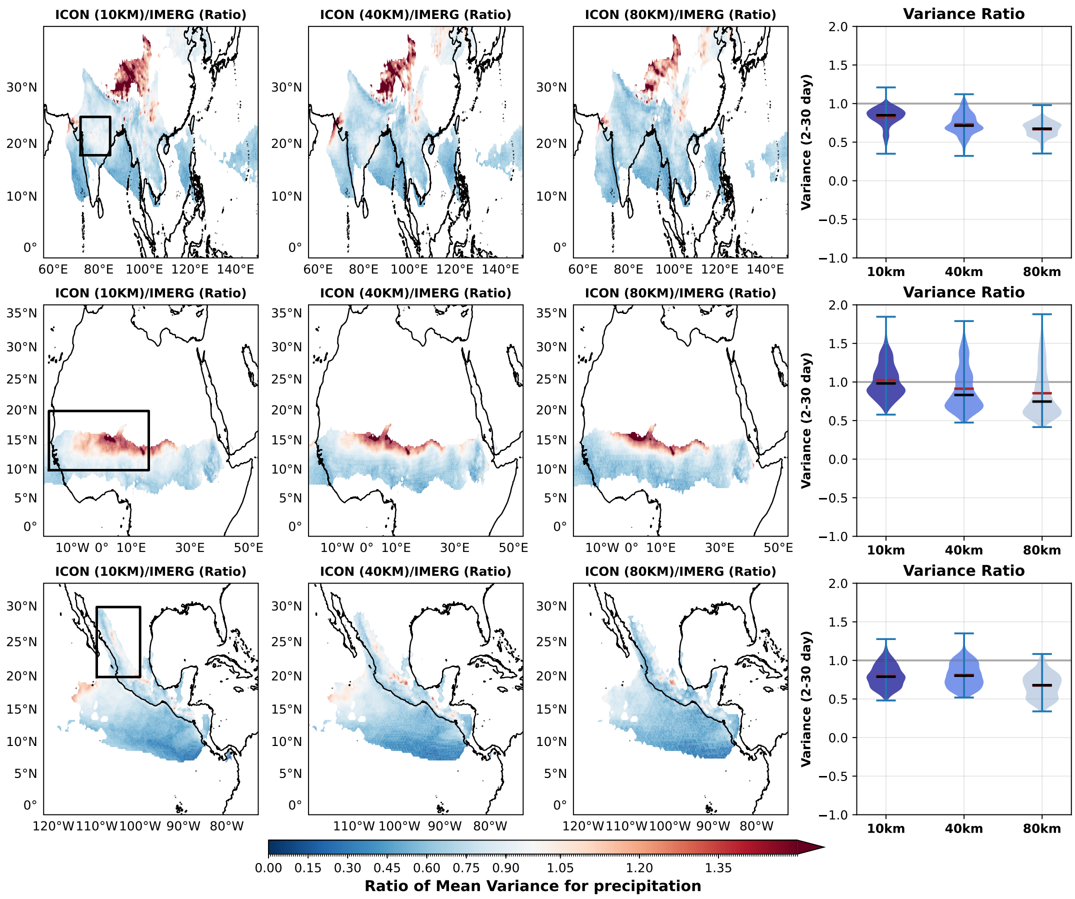

Figure S21: The Spatial patterns of 2–30 day filtered precipitation (transformed with log(1+P)) variance of ICON divided by the variance of IMERG during summer monsoon season (JJAS) representing intraseasonal variability. The top panel shows the ratio of variance for SAsiaM domain, while the region highlighted in the black box represents core monsoon region. Similarly the middle and the bottom panel show WAfriM and NAmerM domains respectively with black box indicating the core monsoon regions. The violin plot on the right most panels show distribution of the variance ratio's in the core monsoon domains, with black bar indicating the median, while the brown bar indicates the mean of the distribution.

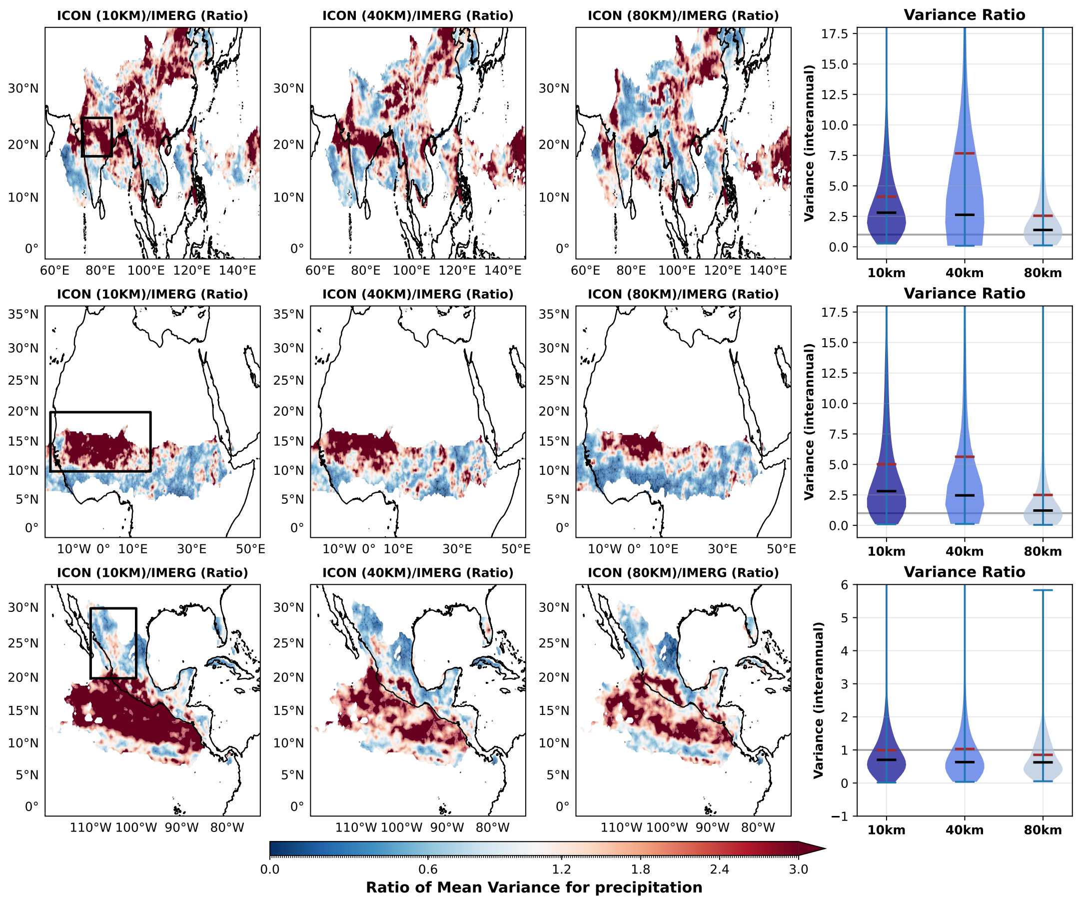

Figure S22: The Spatial patterns interannual variance of ICON divided by the variance of IMERG during summer monsoon season (JJAS) representing intraseasonal variability. The top panel shows the ratio of variance for SAsiaM domain, while the region highlighted in the black box represents core monsoon region. Similarly the middle and the bottom panel show WAfriM and NAmerM domains respectively with black box indicating the core monsoon regions. The violin plot on the right most panels show distribution of the variance ratio's in the core monsoon domains, with black bar indicating the median, while the brown bar indicates the mean of the distribution.